Attempts to perform these complex sequencing experiments are now being examined.

In conclusion, chemical modification of the protein backbone of papain by azobenzene photochromic groups allows photoregulation of the enzyme. Photoinduced isomerization of *trans*-azobenzene groups to *cis*-azobenzene is probably accompanied by structural changes in the protein backbone that affect the binding properties of the enzyme toward the substrate. Further studies that include chemical modification of the enzyme by other photochromic materials and structural characterization of **1**-modified papain are being examined in our laboratory.

Acknowledgment. The support of the Niedersachsen Land Foundation, FRG, is gratefully acknowledged.

Registry No. 1, 37790-20-8; **2**, 37790-19-5; **3**, 131618-74-1; **4**, 37039-24-0; papain, 9001-73-4.

Luminescence Probe and Voltammetry Study of Ion Transport during Redox Switching of Poly(pyrrole) Thin Films

V. Krishna, Y.-H. Ho, S. Basak, and K. Rajeshwar*

Contribution from the Department of Chemistry, Box 19065, The University of Texas at Arlington, Arlington, Texas 76019-0065. *Received August 6, 1990*

Abstract: The ion transport accompanying the redox switching of poly(pyrrole) thin-film electrodes was studied in situ by a new luminescence probe technique. Counterions such as pyrene sulfonate and naphthalene sulfonate, which are fluorescent yet electrochemically silent over the potential window of interest, were used for this purpose. The anodically synthesized poly(pyrrole)–pyrene sulfonate (PP/PS) and poly(pyrrole)–naphthalene sulfonate (PP/NS) thin films were first characterized by cyclic voltammetry. Distinctly different voltammetric fingerprints with associated memory effects were registered for these electrodes depending on the details of the medium in which they were redox cycled. For the in situ study of pseudocathodic processes involving cation transport, positively charged luminescent probes such as $Ru(bpy)_3^{2+}$ (bpy = 2,2′-bipyridyl) and acridine orange hydrochloride were employed. It is shown that the luminescence intensity modulations in the solution phase due to anion or cation transport have different polarities for the electrode potential thus mimicking an electronic (logic) device feature. The temporal aspects of the steady-state luminescence growth were analyzed for the reduction of PP/NS thin films. Diffusion coefficients of 10^{-10}–10^{-11} cm^2/s were thus obtained and were a function of the polymer film thickness. Finally, a novel potential-scan technique combining linear sweep voltammetry with in situ fluorescence monitoring was developed for PP/NS. Only a fraction (2–40%), depending on the potential scan rate and the electrolyte cation, of the total cathodic current resulted in the ejection of the NS^- ions into the fluorometrically sampled solution phase adjacent to the PP/NS thin-film electrodes. The residual current thus is attributed to the competing influence of cation transport into the polymer phase.

Introduction

Polymer-modified electrodes (PME's) have received considerable recent attention stemming in part from their relevance to a variety of application scenarios ranging from electro- and photocatalysis to controlled drug release.[1] Thus, the mechanistic issues related to charge and mass transport in these materials, aside from being fundamentally interesting, have also practical significance. An important mode of charge transport in PME's is recognized to be electron-hopping modeled as a diffusion process with a characteristic coefficient, D_{ct}.[2,3] The electron-hopping process, however, is coupled with counterion motion because of local electroneutrality considerations. The question of whether electron hopping or counterion motion controls the net rate of charge transfer has been addressed for a few PME's of the redox type.[4-6]

Literature precedents for monitoring in situ the mass transport during redox electrochemistry of PME's have been rather limited in range and scope. A major handicap associated with electrochemical probes is that the parameter measured (current, charge, or potential) has little information content of a *chemical* nature. On the other hand, spectroscopic probes have the required sensitivity and, more important, molecular specificity. In a broader context, the importance of the development of in situ probes for the understanding and subsequent optimization of ion transport dynamics in electrochemical situations has been underlined in a recent report.[7] In the spirit that new families of techniques are clearly needed for this purpose, we describe in this paper a luminescence probe technique for the in situ study of ion transport during redox electrochemistry and discuss it within the specific framework of PME's.

This is not the first instance wherein luminescence probes have been used to study PME's. Luminescence from $Ru(bpy)_3^{2+}$ (bpy = 2,2′-bipyridyl) in Nafion-modified electrodes was studied by Buttry and Anson,[8] altnough no attempts were made by these authors to correlate the excited state quenching kinetics with charge/mass transport dynamics. Subsequent studies by Majda and Faulkner[6] illustrate the usefulness of the $Ru(bpy)_3^{2+}$ probe

* Author to whom correspondence should be addressed.

(1) Reviews are contained in: (a) Murray, R. W. In *Electroanalytical Chemistry*; Bard, A. J., Ed.; Dekker: New York, 1984; pp 191–368. (b) Murray, R. W. *Annu. Rev. Mater. Sci.* **1984**, *14*, 145. (c) Faulkner, L. R. *Chem. Eng. News* **1984**, *Feb. 27*, 28. (d) Wrighton, M. S. *Science* **1986**, *231*, 32. (e) Chidsey, C. E. D.; Murray, R. W. *Ibid.* **1986**, *231*, 25. (f) Hillman, A. R. In *Electrochemical Science and Technology of Polymers-1*; Linford, R. G., Ed.; Elsevier: London and New York, 1987; pp 241–291. (g) Murray, R. W.; Ewing, A. G.; Durst, R. A. *Anal. Chem.* **1987**, *59*, 379A.

(2) For example: (a) Dahms, H. *J. Phys. Chem.* **1968**, *72*, 362. (b) Ruff, I.; Friedrich, V. J. *Ibid.* **1971**, *75*, 3297.

(3) (a) Saveant, J.-M. *J. Electroanal. Chem.* **1986**, *201*, 211. (b) Saveant, J.-M. *Ibid.* **1986**, *238*, 1. (c) Saveant, J.-M. *J. Phys. Chem.* **1988**, *92*, 1011. (d) Andrieux, C. P.; Saveant, J.-M. *Ibid.* **1988**, *92*, 6761.

(4) (a) Ikeda, T.; Schmehl, R.; Denisevich, P.; Willman, K.; Murray, R. W. *J. Am. Chem. Soc.* **1982**, *104*, 2683. (b) Ikeda, T.; Leidner, C. R.; Murray, R. W. *J. Electroanal. Chem.* **1982**, *138*, 343.

(5) White, H. S.; Leddy, J.; Bard, A. J. *J. Am. Chem. Soc.* **1982**, *104*, 4811.

(6) (a) Majda, M.; Faulkner, L. R. *J. Electroanal. Chem.* **1982**, *137*, 149. (b) Majda, M.; Faulkner, L. R. *Ibid.* **1984**, *169*, 77.

(7) Faulkner, L. R., Ed. In Situ Characterization of Electrochemical Processes, NMAB-438-3; National Materials Advisory Board, National Research Council: Washington, DC, 1987.

(8) Buttry, D. A.; Anson, F. C. *J. Am. Chem. Soc.* **1982**, *104*, 4824.

0002-7863/91/1513-3325$02.50/0

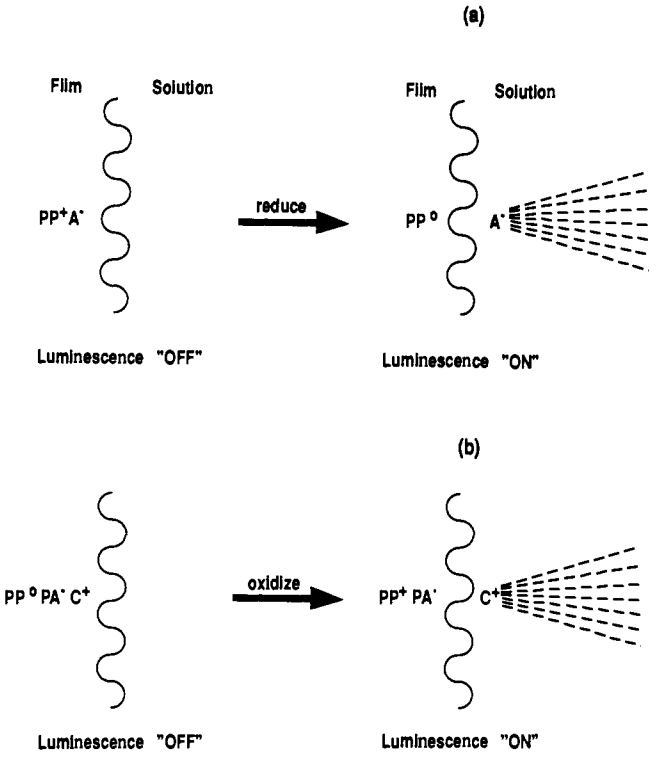

Figure 1. Scheme for in situ luminescence monitoring of ion transport during redox electrochemistry of a poly(pyrrole)-modified electrode. Upper: Strategy for monitoring anion transport—A^- refers to an anionic luminescence probe. Lower: Strategy for monitoring cation transport in a pseudocathodic doping process—PA^- refers to a polyanionic electrolyte and C^+ is a positively charged luminescence probe.

in shedding light on the dynamics of electron diffusion in poly(styrenesulfonate)-modified electrodes. Coordinatively attached luminescent probes also have been employed for the study of local environments in poly(4-vinylpyridine)-modified electrodes.[9] We further note related studies on the use of luminescent molecules for polymer systems in general, albeit as probes of the microenvironment rather than charge/mass transport.[10]

Our method, schematized in Figure 1, fundamentally differs from the above approaches in that the measurements are confined to the solution (rather than to the electrode) phase. This leads to a considerable interpretative advantage given the propensity of light-scattering, inner-filter, and quenching effects on luminescence from solid surfaces. Further, we choose suitable (electrochemically silent) luminescent species as the counterions. In this regard, our strategy is an extension of the one we previously employed to study electrochemically induced pH modulations at RuO_2- and poly(pyrrole)–electrolyte interphases.[11,12]

We have chosen to demonstrate our technique using poly(pyrrole) as a model system. This polymer has been a popular model for studies on PME's of the electronically conductive type.[13-17] The ability to redox switch such materials from the insulating state to an electronically conductive form is crucial to many projected applications of PME's. The associated ion fluxes could be either predominantly anionic or cationic depending on the chemical architecture and other properties of the particular poly(pyrrole) sample.[11,18-22] Both these scenarios are illustrated in Figure 1. We will show how our luminescent probe strategy is applicable to both types of situations by judicious choice of the probe moiety. Our ability to modulate the luminescent property in a predictable manner via simple control of an electrode potential (or current) may be important in itself,[23] as for example, in chemical sensing applications. Additionally, as experimentally demonstrated below, the luminescence ON–OFF "logic states" for the anion and cation situations in Figure 1 have different polarities mimicking an electronic device feature.

Our strategy (Figure 1a) relies on the use of a luminescent ion which also serves the dual purpose of a dopant or counterion for oxidized poly(pyrrole). Thus, two representative species, namely pyrene sulfonate and naphthalene sulfonate, were used in this study. The resultant poly(pyrrole) thin films were characterized in some detail by cyclic voltammetry (CV). We will show in particular that CV is a powerful technique for the in situ monitoring of evolving changes in the polymer thin film composition as the electrode is cycled in various electrolytes. Novel memory effects will be described with this technique. To evaluate the feasibility of the luminescence probe technique for studying cation transport, we have employed poly(pyrrole) thin films containing a polyelectrolyte [e.g., poly(styrenesulfonate)] in order to "freeze" the anion motion.[24] Use of *positively charged* luminescence probes (e.g., $Ru(bpy)_3^{2+}$, acridine orange hydrochloride), in this case, enables the acquisition of a modulated signal which is tuned to the cation transport (Figure 1b).

Finally, we will demonstrate a novel potential-scanning technique which combines linear sweep voltammetry (LSV) with in situ fluorometric monitoring of the ion transport at the PME/electrolyte interphase. These experiments reveal that the amount of dopant anions fluorometrically sampled in the solution phase adjacent to the PME is often much less than that expected from the charge consumed in the polymer reduction. The possible reasons for this, which may have implications in the practical use of these PME's (e.g. in batteries), are discussed.

Our luminescence probe approach was briefly described in an

(9) (a) Oh, S.-M.; Faulkner, L. R. *J. Am. Chem. Soc.* **1989**, *111*, 5613. (b) Oh, S.-M.; Faulkner, L. R. *J. Electroanal. Chem.* **1989**, *269*, 77.

(10) (a) Rasmussen, J. R.; Bergbreiter, D. E.; Whitesides, G. M. *J. Am. Chem. Soc.* **1977**, *99*, 4746. (b) Lee, P. C.; Meisel, D. *Ibid.* **1980**, *102*, 5477. (c) Rice, M. R.; Gold, H. S. *Anal. Chim. Acta* **1984**, *164*, 111. (d) Herkstoeter, W. G. *J. Polym. Sci. (Polym. Chem. Ed.)* **1984**, *22*, 2395. (e) Alvarez-Roa, E. R.; Prieto, N. E.; Martin, C. R. *Anal. Chem.* **1984**, *56*, 1939. (f) Holmes-Farley, S. R.; Whitesides, G. M. *Langmuir* **1986**, *2*, 266. (g) Blatt, E.; Launikonis, A.; Mau, A. W.-H.; Sasse, W. H. F. *Aust. J. Chem.* **1987**, *40*, 1. (h) Blatt, E.; Sasse, W. H. F.; Mau, A. W.-H. *J. Phys. Chem.* **1988**, *92*, 4151.

(11) Tsai, E. W.; Jang, G.-W.; Rajeshwar, K. *J. Chem. Soc., Chem. Commun.* **1987**, 1776.

(12) (a) Jang, G.-W.; Tsai, E. W.; Rajeshwar, K. *J. Electrochem. Soc.* **1987**, *134*, 2377. (b) Jang, G.-W.; Tsai, E. W.; Rajeshwar, K. *J. Electroanal. Chem.* **1989**, *263*, 383.

(13) Review: Chandler, G. K.; Pletcher, D. *Spec. Period. Rep., Electrochem.* **1985**, *10*, 117–150.

(14) (a) Bull, R. A.; Fan, F.-R. F.; Bard, A. J. *J. Electrochem. Soc.* **1982**, *129*, 1009. (b) Bull, R. A.; Fan, F.-R. F.; Bard, A. J. *Ibid.* **1983**, *130*, 1636. (c) Fan, F.-R. F.; Bard, A. J. *Ibid.* **1986**, *133*, 301. (d) Castro-Acuna, C. M.; Fan, F.-R. F.; Bard, A. J. *J. Electroanal. Chem.* **1987**, *234*, 347. (e) Nagasubramanian, G.; DiStefano, S.; Moacanin, J. *J. Phys. Chem.* **1986**, *90*, 4447. (f) Lee, C.; Kwak, J.; Bard, A. J. *J. Electrochem. Soc.* **1989**, *136*, 3720. (g) Kwak, J.; Lee, C.; Bard, A. J. *Ibid.* **1990**, *137*, 1481.

(15) (a) Burgmayer, P.; Murray, R. W. *J. Am. Chem. Soc.* **1982**, *104*, 6139. (b) Burgmayer, P.; Murray, R. W. *J. Phys. Chem.* **1984**, *88*, 2515. (c) Feldman, B. J.; Burgmayer, P.; Murray, R. W. *J. Am. Chem. Soc.* **1985**, *107*, 872. (d) McCarley, R. L.; Morita, M.; Wilbourn, K. O.; Murray, R. W. *J. Electroanal. Chem.* **1988**, *245*, 321.

(16) (a) Miller, L. L.; Zinger, B.; Zhou, Q.-X. *J. Am. Chem. Soc.* **1987**, *109*, 2267. (b) Zhou, Q.-X.; Miller, L. L.; Valentine, J. R. *J. Electroanal. Chem.* **1989**, *261*, 147.

(17) (a) Kittlesen, G. P.; White, H. S.; Wrighton, M. S. *J. Am. Chem. Soc.* **1984**, *106*, 7389. (b) Shu, C.-F.; Wrighton, M. S. *J. Phys. Chem.* **1988**, *92*, 5221.

(18) Kaufman, J. H.; Kanazawa, K. K.; Street, B. *Phys. Rev. Lett.* **1984**, *53*, 2461.

(19) Zhou, Q.-X.; Kolaskie, C. J.; Miller, L. L. *J. Electroanal. Chem.* **1987**, *223*, 283.

(20) Pickup, P. G. *J. Electroanal. Chem.* **1987**, *225*, 273.

(21) (a) Sundaresan, N. S.; Basak, S.; Pomerantz, M.; Reynolds, J. R. *J. Chem. Soc., Chem. Commun.* **1987**, 621. (b) Reynolds, J. R.; Sundaresan, N. S.; Pomerantz, M.; Basak, S.; Baker, C. K. *J. Electroanal. Chem.* **1988**, *250*, 355. (c) Basak, S.; Rajeshwar, K.; Kaneko, M. *Anal. Chem.* **1990**, *62*, 1407.

(22) (a) Bidan, G.; Ehui, B.; Lapkowski, M. *J. Phys. D: Appl. Phys.* **1988**, *21*, 1043. (b) Ikenoue, Y.; Chiang, J.; Patil, A. O.; Wudl, F.; Heeger, A. J. *J. Am. Chem. Soc.* **1988**, *110*, 2983. (c) Ikenoue, Y.; Uotani, N.; Patil, A. O.; Wudl, F.; Heeger, A. J. *Synth. Met.* **1989**, *30*, 305.

(23) Tsai, E. W.; Phan, L.; Rajeshwar, K. *J. Chem. Soc., Chem. Commun.* **1988**, 771.

(24) (a) Miller, L. L.; Zhou, Q. X. *Macromolecules* **1987**, *20*, 1594. (b) Shimidzu, T.; Ohtani, A.; Iyoda, T.; Honda, K. *J. Electroanal. Chem.* **1987**, *224*, 123.

earlier communication.[25] We elaborate on these and other new results in this full paper.

Experimental Section

Chemicals and Equipment. Pyrrole, lithium perchlorate, tetraethylammonium *p*-toluenesulfonate (TEAOTs), sodium 2-naphthalenesulfonate (NaNS), acridine orange hydrochloride [3,6-bis(dimethylamino)acridine hydrochloride], and poly(sodium 4-styrenesulfonate) (NaPSS) were Aldrich. Sodium 1-pyrenesulfonate (NaPS) and Ru(bpy)$_3$Cl$_2$·6H$_2$O were procured from Molecular Probes, Inc. and G. Frederick Smith, respectively. Tetrabutylammonium perchlorate (TBAP), tetrabutylammonium fluoroborate (TBABF$_4$), and tetrabutylammonium fluorophosphate (TBAPF$_6$) were from Southwestern Analytical Chemicals. Pyrrole was purified by distillation and the other chemicals by recrystallization usually from acetone–methanol (J. T. Baker) mixtures. Acetonitrile (Fisher Scientific, spectroscopic grade) was distilled over P_2O_5 and dried with Al_2O_3 prior to use. Deionized water was from a Corning Megapure system.

Electrochemical experiments were performed either on an EG&G Princeton Applied Research (PAR) System equipped with Model 173, 175, and 179 modules and a Model RE 0074 *x–y* recorder or on a Bioanalytical Systems (BAS) Model 100A electrochemical analyzer which was interfaced with an IBM PC/XT. Luminescence experiments utilized a Perkin-Elmer MPF-44B spectrofluorometer. A Tencor Alfastep profilometer was employed for thin film thickness measurements. X-ray photoelectron spectroscopy (XPS) was performed on a Physical Electronics Model 5000C system fitted with a Al anode. Both as-synthesized thin-film electrodes and those voltammetrically reduced in 0.1 M $MClO_4$ electrolyte (M = Li, Na, K, and Cs) were compared for their relative cation uptake.

Cells and Accessories. The electrochemical cell design for CV and polymer thin-film growth was of standard single-compartment three-electrode design. Either Pt foil (Alfa) or disks (BAS or III Supplies) were used as the substrate for the PME's. The Pt surface was first polished with 0.3-μm Al_2O_3 (Buehler) followed by pretreatment via established procedures.[26] A Pt wire (Aesar) was used as the counter-electrode for the various experiments described below. An Ag/AgCl reference electrode was employed for the thin film growth experiments. Cyclic voltammetry and luminescence spectroelectrochemistry employed either a Ag or a Pt quasireference electrode. These were carefully calibrated with either ferrocene (for the nonaqueous solvents) or Fe(CN)$_6^{3-/4-}$ redox couples (for the aqueous electrolytes). For ease of comparison, however, all the potentials below are quoted with reference to the Ag/AgCl reference unless otherwise noted.

The luminescence spectroelectrochemical cell was a modification of the one used in a previous study.[23] Many of the features in the design reported by previous authors[27] were also incorporated. Particular care was taken to align the excitation light beam away from the poly(pyrrole) surface to avoid primary inner filter effects. It is important to note, in the discussion that follows, that the luminescence originates entirely in the solution contacting the polymer surface.

Polymer Thin-Film Growth and Procedures. The poly(pyrrole) dopant ion combination will be designated in what follows as PP/dopant. Thus, a poly(pyrrole) thin film containing naphthalenesulfonate as the dopant is shown as "PP/NS". The poly(pyrrole) thin films were anodically electrosynthesized by a potential-step technique. Nominal growth conditions were the following: +900 mV, 0.1 M of pyrrole and 0.1 M of the dopant anion. Similar conditions were employed for poly(pyrrole) thin films containing a polyelectrolyte as the counterion, namely PP/PSS. The thickness of the polymer thin films was controlled via the anodic coulombs passed. Charge–thickness correlations were established via independent thin-film profilometry measurements (see above). A representative plot for the PP/NS system is contained in Figure 2. The slope of this plot yields a factor of 5.7 μm C^{-1} cm^2.

This factor as reported in previous studies has been somewhat variable, stemming undoubtedly from the dependence of the coulombic efficiency for the polymerization on experimental variables such as monomer concentration, dopant anion, electrolyte composition, substrate, etc. For example, the quoted factors (in μm C^{-1} cm^2) include 2.50,[18] 4.16,[14a,28] 2.64,[29] 2.75,[30a] and 2.5.[21c] It is interesting that much higher efficiencies

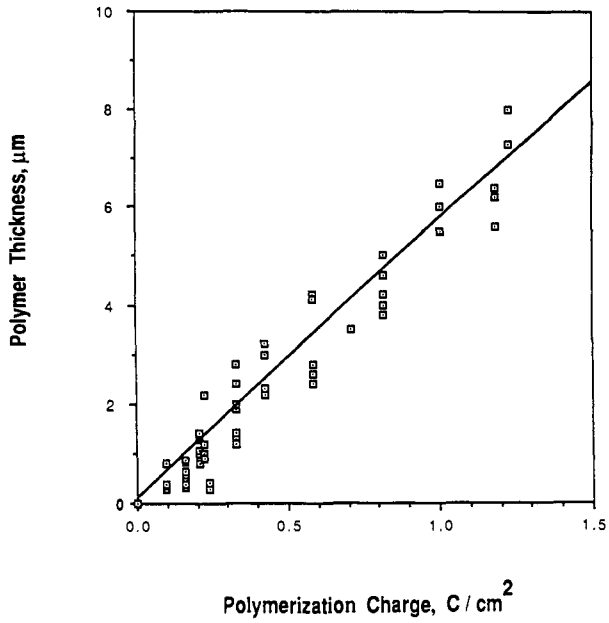

Figure 2. Plot of the poly(pyrrole) film thickness as determined by stylus profilometry vs the coulombs passed during the anodic polymerization. These data are for the PP/NS thin films (refer to the text for electrode notation). The replicate measurements were done by scribing different portions of the same sample. The line is a least-squares fit.

(even higher than what we have seen here for our samples) are afforded by indium tin oxide substrates for which factors of 6.85 and 6.1 have been reported.[21c,30b]

Our PP/PS thin films yielded conversion factors very similar to that quoted above for the PP/NS case (Figure 2). For PP/PSS, we used a value of 2.5.[21c] All the polymer thin films in this study were grown from aqueous media.

The PP/NS and PP/PS electrodes thus prepared were removed from the polymerization medium after the requisite number of coulombs had been passed. [These electrodes were returned to the open-circuit (rest) condition (ca. −185 mV) prior to removal.] The trapped NS$^-$ and PS$^-$ from the polymer thin film (which presumably occurred during film growth) were removed by thorough rinsing in H_2O and MeCN. The efficacy of this procedure was checked with fluorescence assay of the washings. The absence of a signal due to NS$^-$ and PS$^-$ was taken to indicate complete removal of *absorbed* NS$^-$ and PS$^-$ prior to CV and luminescence spectroelectrochemistry. Of course, any *specifically adsorbed* NS$^-$ and PS$^-$ (i.e., those ions held within the double-layer at the interphase) presumably are not affected; these in turn manifest in the subsequent CV and luminescence analyses to be described below.

The excitation wavelength was kept fixed in all the luminescence spectroelectrochemistry experiments. The spectral band-pass (SB) was either 4 or 8 nm. In the modulation-type experiments (Figure 7), the emission spectrum was scanned with the SB set at 2 nm. All the luminescence emission spectra shown below are uncorrected. In the potential-scanned mode (Figure 10) both excitation and emission wavelengths were kept fixed, and to secure a higher S/N ratio, wider slit widths (SB 6–8 nm) were employed for the excitation light. In this case, the trigger on the potentiostat was used to initiate digital data acquisition on the PC/XT using a D/A board (Data Translation Inc.). These experiments were performed on the PP/NS system as a demonstration example. The amount of NS$^-$ ejected from the polymer thin film (cf. Figure 10 below) was computed from a control calibration run obtained under identical conditions. A solution of $LiClO_4$ in the luminescence spectroelectrochemical cell was spiked with incremental volumes of NaNS standards prepared in 0.1 M $LiClO_4$ for this purpose.

All aqueous electrolyte-based measurements employed N_2 purging to remove traces of O_2. Experiments utilizing nonaqueous electrolytes either employed an Ar drybox (Vacuum Atmospheres) or, in some cases, simply a N_2 blanket. In all the cases, however, the MeCN solvent and the supporting electrolytes were carefully stored in an inert atmosphere. Long-term exposure of the synthesized PP/NS and PP/PS samples to the ambient in the dry state was also avoided because of concerns with

(25) Basak, S.; Ho, Y.-H.; Tsai, E. W.; Rajeshwar, K. *J. Chem. Soc., Chem. Commun.* **1989**, 462.
(26) Adams, R. N. *Electrochemistry at Solid Electrodes*; Dekker: New York, 1969; Chapter 7, p 187.
(27) Turner-Jones, E. T.; Faulkner, L. R. *J. Electroanal. Chem.* **1984**, *179*, 53.
(28) Diaz, A. F.; Castillo, J. I. *J. Chem. Soc., Chem. Commun.* **1980**, 397.
(29) Penner, R. M.; Van Dyke, L. S.; Martin, C. R. *J. Phys. Chem.* **1988**, *92*, 5274.
(30) (a) Aoki, K.; Tezuka, Y.; Shinozaki, K.; Sato, H. *Denki Kagaku* **1989**, *57*, 397. (b) Tezuka, Y.; Aoki, K.; Shinozaki, K. *Synth. Met.* **1989**, *30*, 369.

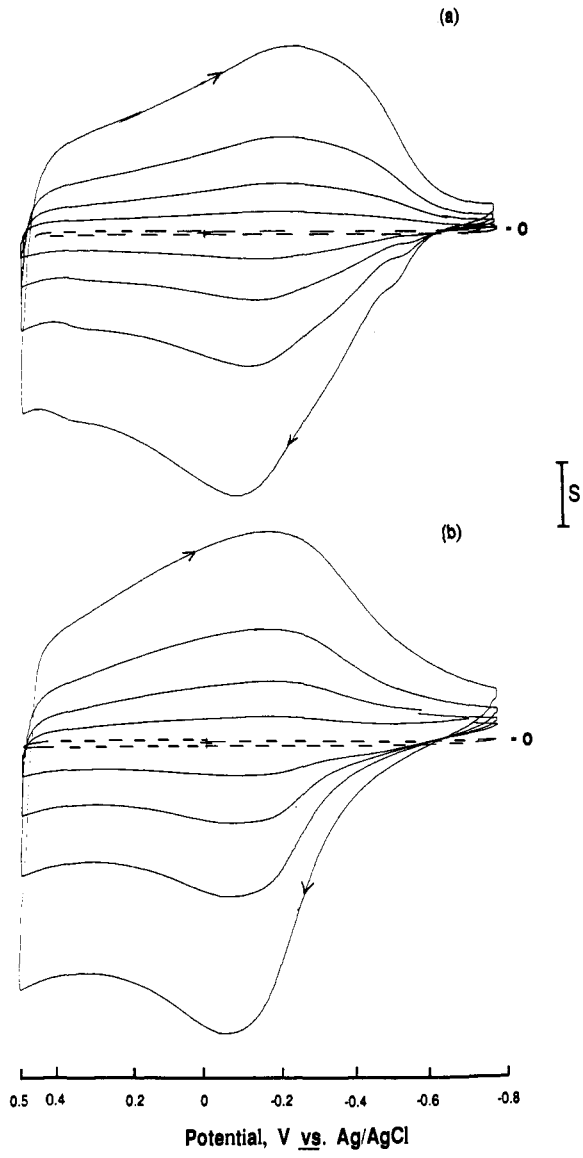

Figure 3. Cyclic voltammograms for Pt-supported PP/NS (a) and PP/PS (b) thin-film electrodes in 0.1 M TBAP, MeCN as a function of the scan rate (20, 50, 100, and 200 mV/s). The corresponding voltammograms for the Pt substrate are shown by a dashed line in each case for a scan rate of 200 mV/s. The current scale is 6.25 and 1 μA in parts a and b, respectively.

their chemical stability. Freshly prepared thin films were used for each experiment for this reason. All measurements below pertain to ambient laboratory temperature.

Results and Discussion

Cyclic Voltammetry of PP/NS and PP/PS Thin-Film Electrodes. Cyclic voltammetry (CV) has been a powerful tool for characterizing the redox beavior of poly(pyrrole)-modified electrodes. Thus, Diaz et al.[31] observe oxidation and reduction waves at ~−80 and −300 mV (vs SSCE reference), respectively, for their PP/BF_4 thin films in $TEABF_4$/MeCN. The influence of both electrolyte cations (TMA^+, TEA^+, TBA^+, THA^+) and anions (ClO_4^-, BF_4^-, PF^{6-}) on the redox behavior was investigated by these authors. The observed effects (peak splitting, potential shifts) on the redox behavior were ascribed to solubility, ion mobility, and ion pairing differences between the various salts. Similar peak-splitting effects have been noted by Kuwabata et al.[32] for MeCN-synthesized PP/ClO_4 thin films in aqueous electrolytes containing Li^+, Na^+, and K^+ and Cl^-, Br^-, I^-, ClO_4^-, SO_4^{2-}, HPO_4^{2-}, and WO_4^{2-}. Interestingly enough, these authors observe anodic peak splitting only for divalent anionic species—an effect they ascribe to a multistep oxidation sequence involving surface and bulk insertion modes into the polymer, respectively. Attempts

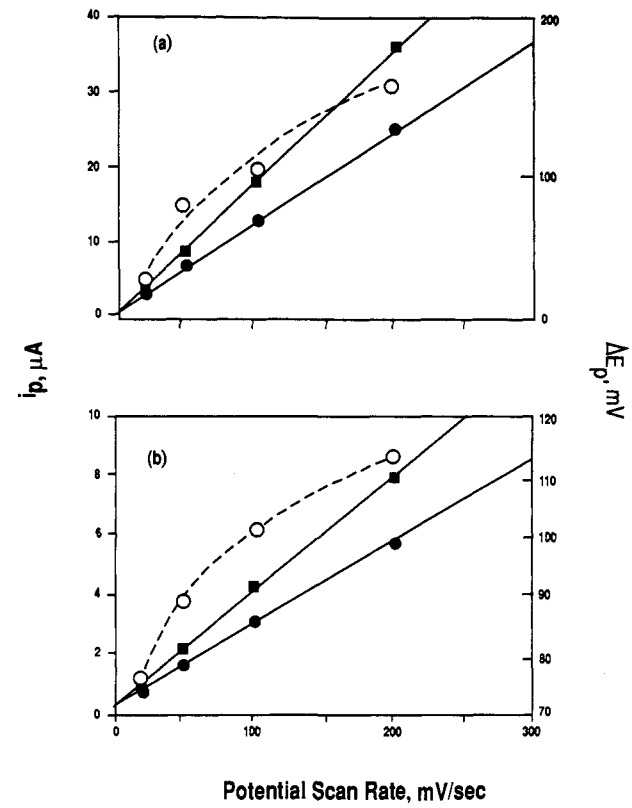

Figure 4. Variation of the CV parameters for the data in Figure 3 for PP/NS (a) and PP/PS (b). Trends for both the peak currents, i_p, for the anodic (■) and cathodic (○) waves as well as the peak potential separation, ΔE_p (○), are shown.

to correlate the incorporated anion with the redox voltammetric fingerprints have been made by Shimidzu et al.[24b] In addition to KCl and $KClO_4$, these authors used a series of sulfonate salts of Na (varying in size from ethanesulfonate to PSS^-) in aqueous media to synthesize their poly(pyrrole) thin films. Subsequent cycling of these electrodes, again in aqueous media, enabled correlation of their redox activity with anion mobility and coupled cation transport phenomena (cf. Figure 1). It is interesting to note the positive location of the redox waves for the thin films in this study (e.g., E_{pa} = +250 mV and E_{pc} = +80 mV vs SCE reference for PP/Cl) relative to the observations in the preceding two studies.[31,32] A negative potential shift is generally observed for both oxidation and reduction waves in the sulfonate-containing cases.[24b] A similar set of electrolytes has been very recently employed by Vork et al.[33] for the synthesis of supported and self-standing poly(pyrrole) thin films, although no voltammetric data were reported by these authors.

The above findings prompted us to examine the voltammetric behavior of our PP/NS and PP/PS electrodes in various electrolytes and solvents. The behavior of these two systems was not sufficiently distinct to warrant separate discussion; thus the PP/NS thin films are mainly described below. *In the ensuing discussion, it must be recognized that the potential range that we have chosen for voltammetric scanning is such that both NS^- and PS^- are electrochemically silent.*

Figure 3 contains cyclic voltammograms for PP/NS (Figure 3a) and PP/PS (Figure 3b) in 0.1 M TBAP, MeCN with the potential scan rate, v, as a variable. (This notation is hereafter employed to designate the supporting electrolyte, solvent combination.) The E_{pa}'s for both systems occur around −160 mV with E_{pc} shifted somewhat more negative to ~−240 and −200 mV for

(31) Diaz, A. F.; Castillo, J. I.; Logan, J. A.; Lee, W.-Y. *J. Electroanal. Chem.* **1981**, *129*, 115.
(32) Kuwabata, S.; Yoneyama, H.; Tamura, H. *Bull. Chem. Soc. Jpn.* **1984**, *57*, 2247.
(33) Vork, F. T. A.; Schuermans, B. C. A. M.; Barendrecht, E. *Electrochim. Acta* **1990**, *35*, 567.

PP/NS and PP/PS, respectively. The peak separation, ΔE_p, essentially disappears at $v \leq 10$ mV/s although the definition of the redox waves on the "capacitive" background envelope (see below) is much attenuated in this regime. The variation of ΔE_p and the peak currents i_{pa}, i_{pc} with v for the two cases is shown in Figure 4. The overall trends are consistent with reasonably facile charge transport in these PME's, especially when they are voltammetrically cycled in electrolytes containing ClO_4^- and similar ions, see below.

We observe an oxidation pre-peak in some samples (cf Figure 3a); the origin of such a pre-peak has been the subject of a recent paper.[34] Experimental data were also shown by these authors for poly(aniline).

Although PP/NS has been the subject of morphological and conductivity examinations by previous authors,[35,36] we are not aware of substantive voltammetric studies on this material. The other system, namely, PP/PS as far as we know, is new. What happens to the voltammetric profiles when these electrodes are cycled in other electrolytes and solvents? This question is taken up next with PP/NS as a model system. For comparison, we also performed a few experiments with PP/OTs.[37]

After thin-film growth, the PP/NS electrodes were transferred to a new cell as described in the Experimental Section. The scan was initiated in each case from either 0 V or +150 mV in the negative direction up to −900 mV, then in the positive-going direction up to +500 mV, and finally back to the initial potential. A 0.1 M solution of the electrolyte in either MeCN or H_2O was employed. During this sequence, the NS^- species are first ejected from the polymer and subsequently replaced by the solvent electrolyte species in the anodic cycle (cf. Figure 1a). The latter process is dominated by the solvent species because of the imbalance in the relative concentrations (0.1 vs $\sim 10^{-8}$ M of NS^- in the polymer). The end result is a gradual evolution in the polymer thin-film composition from the (initial) PP/NS one to the PP/X state with repeated cycling. In each case, the first cathodic scan evinces a sharp reduction wave signalling the rather drastic morphology change which the PME initially has to undergo to accommodate the ingressing anion. (An alternative scenario involving electrolyte cations already has been discussed (Figure 1b); this situation dominates in some of the cases described below.)

The voltammetric data presented below pertain to PP/NS thin films thus "exercised" for an initial cycle. The stability thereafter is rather good although some minor alterations in the profiles often occur as illustrated by the examples in Figure 5, traces a and c, respectively. Consider Figure 5a for a PP/NS thin film cycled in TBAP, MeCN. This voltammogram is not markedly different from that in Figure 3a. Very similar traces were obtained with $TBAPF_6$, MeCN and $TBABF_4$, MeCN (not shown). This trend is interpretable on the basis of the rather negligible solvation of these anions in MeCN and their comparable Stokes radii: $r(ClO_4^-) = 0.232$ nm, $r(PF_6^-) = 0.233$ nm, and $r(BF_4^-) = 0.222$ nm.[38] Further, $LiClO_4$, MeCN yields similar voltammetric profiles (not shown), indicating that cation transport is not predominant, at least in this case. The voltammogram in Figure 5b (curve 1) for TEAOTs, MeCN, on the other hand, shows interesting differences in that the "capacitive" envelope (see below) at the positive potential end is diminished and the oxidation wave shifts positive and further splits into a doublet.

More drastic variations in the voltammetric fingerprint result for PP/NS cycled in NaPSS, H_2O (Figure 5c) and NaNS, H_2O

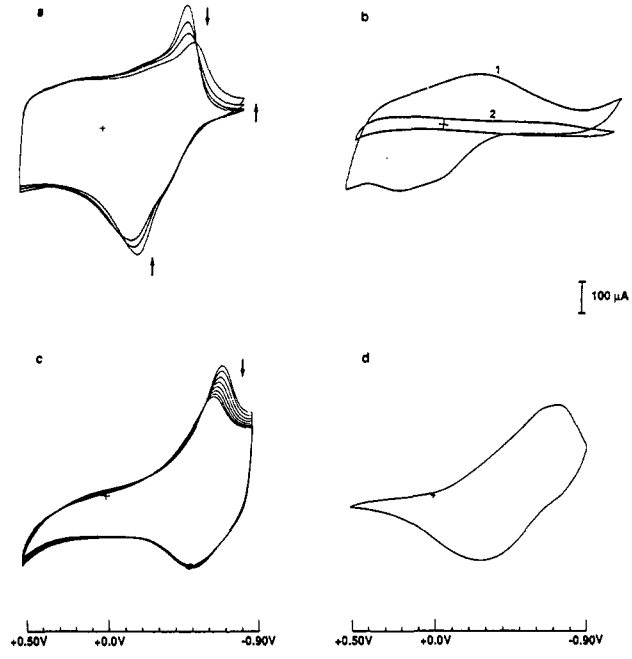

Figure 5. The CV traces (scan rate 50 mV/s) for PP/NS thin-film electrodes in TBAP, MeCN (a); TEAOTs, MeCN (curve 1, b); TEAOTs, H_2O (curve 2, b); NaPSS, H_2O (c); and NaNS, H_2O (d). The electrolyte concentration was 0.1 M in each case; the scan was initiated from either +0.15 or 0 V in the negative direction first. The first "exercise" cycle (refer to text) is not shown. The subsequent gradual changes in the voltammogram morphology typically are as shown in parts a and c, wherein the arrows denote the direction of evolution of the change. Different PP/NS samples were utilized in parts a → d; the polymer was ca. 0.3 μm thick.

(Figure 5d), respectively. Note the relative lack of prominence of the capacitive envelope in the 0 to +500 mV window in these cases and the shift of the polymer redox activity to more negative potentials. Finally, a PP/NS electrode cycled in TEAOTs, H_2O shows little redox or electroactive behavior (curve 2, Figure 5b).

These voltammetric trends with the different electrolytes and solvents are stable and reproducible and have been confirmed by measurements on a large number of PP/NS samples. *More important, it is possible to repeatedly and reversibly induce transitions from one voltammogram morphology to the other in Figure 5.* Another graphic illustration of this "memory effect" is furnished by the sequence of voltammetric scans in Figure 6. The starting PME in this case was a PP/OTs thin film. This electrode was scanned as before in TEAOTs, H_2O yielding a voltammogram (Figure 6a) similar to that contained in Figure 5b, curve 2. This electrode was taken out and rinsed after the scan was terminated at the initial potential. Transfer to TBAP, MeCN and scanning, *this time from a negative limit* (∼−850 mV), yielded the voltammogram in Figure 6b. A second repeat cycle of electrolyte and solvent switching in this manner yields the set of voltammograms in Figure 6, c and d, for TEAOTs, H_2O and TBAP, MeCN, respectively. The loss of electroactivity in TEAOTs, H_2O clearly is not permanent, and the alterations in the voltammetric profiles are reversible in terms of the gross features (subtle differences do exist as suggested by a comparison of parts b and d in Figure 6).

Aside from the solvent and electrolyte factors discussed above (solubility, ion mobility, ion pairing), the sensitivity of the voltammogram morphology may be additionally interpreted within the framework of film swelling, structure change,[39] and lipophilicity[40] effects. Another interesting trend that emerges from

(34) Gottesfeld, S.; Redondo, A.; Rubinstein, I.; Feldberg, S. W. *J. Electroanal. Chem.* **1989**, *265*, 15.

(35) (a) Buckley, L. J.; Roylane, D. K.; Wnek, G. E. *J. Polym. Sci. B: Polym. Phys.* **1987**, *25*, 2179. (b) Yamaura, M.; Haginara, T.; Iwata, K. *Synth. Met.* **1988**, *26*, 209. (c) Mitchell, G. R.; Davis, F. J.; Legge, C. H. *Ibid.* **1988**, *26*, 247. (d) Warren, L. F.; Anderson, D. P. *J. Electrochem. Soc.* **1987**, *134*, 101. (e) Warren, L. F.; Walker, J. A.; Anderson, D. P.; Rhodes, C. G.; Buckley, L. J. *Ibid.* **1989**, *136*, 2286.

(36) (a) Kuwabata, S.; Okamoto, K.; Ikeda, O.; Yaneyama, H. *Synth. Met.* **1987**, *5*, 157. (b) Kuwabata, S.; Okamoto, K.; Yoneyama, H. *J. Chem. Soc., Faraday Trans. 1* **1988**, *84*, 2317.

(37) Wynne, K. J.; Street, G. B. *Macromolecules* **1985**, *18*, 2361.

(38) Visy, C. S.; Lukkari, J.; Pajunen, T.; Kankara, J. *Synth. Met.* **1989**, *33*, 289.

(39) (a) Heinze, J.; Bilger, R.; Meerholz, K. *Ber. Bunsenges. Phys. Chem.* **1988**, *92*, 1271. (b) Heinze, J.; Dietrich, M.; Mortensen, J. *Makromol. Chem., Macromol. Symp.* **1987**, *8*, 73.

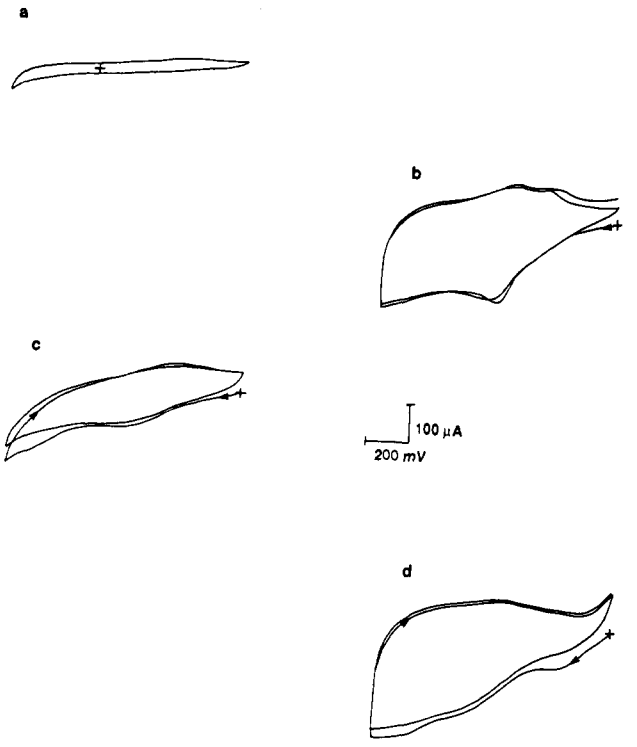

Figure 6. An example of a "memory effect" in the voltammetric behavior of a PP/OTs thin film. The CV traces were acquired between −0.85 and +0.50 V each in 0.1 M electrolyte which was sequentially altered (refer to text) in the following order: (a) TEAOTs, H_2O; (b) TBAP, MeCN; (c) TEAOTs, H_2O; and (d) TBAP, MeCN. Note that the same electrode was used in these experiments, the polymer film was ca. 0.4 μm thick, and the scan was initiated in the positive-going direction from the negative limit, namely, −0.85 V.

the voltammetric data in Figure 5 and 6 is that the "capacitive" envelope between 0 and +500 mV appears to be pronounced only in the cases where anion transport (cf. Figure 1a) is an important mass transport pathway (e.g., in Figure 5 compare part a with parts c and d). We thus view this envelope as a manifestation of the progressive uptake of anions by the polymer as more and more positive charge is injected into it.

Luminescence Modulation Experiments of PP/NS, PP/PS, and PP/PSS. It obviously is important to first establish that the luminescence probe approach (cf. Figure 1) is a faithful indicator of the ion fluxes during redox electrochemistry of poly(pyrrole) thin films. To this end, we performed a series of experiments on PP/NS and PP/PS thin films; the corresponding data are contained in Figures 7–9.

Before discussing these data, a few words about the NaNS and NaPS fluorescence probes themselves may be in order. In terms of the objectives of this study, their main attribute is that they contain both a photophysical hydrocarbon core as well as the $-SO_3^-$ dopant ion functionality. Both naphthalene and pyrene along with their derivatives have been popular probes for microenvironmental effects such as local polarity etc.[10] The NaNS probe on fluorescence excitation at 284 nm reveals an emission spectrum comprising two distinct peaks at 326 and 340 nm, respectively. Better vibronic fine structure is evident with NaPS, which on excitation at 330 nm shows a set of four bands between 350 and 500 nm (cf. Figure 7 below).[10g] The vibronic fine structure is even more pronounced for pyrene itself underlining its utility as an environmental probe.[41]

Figure 7a contains a sequence of fluorescence emission spectra of the solution adjacent to a PP/PS thin-film electrode held at

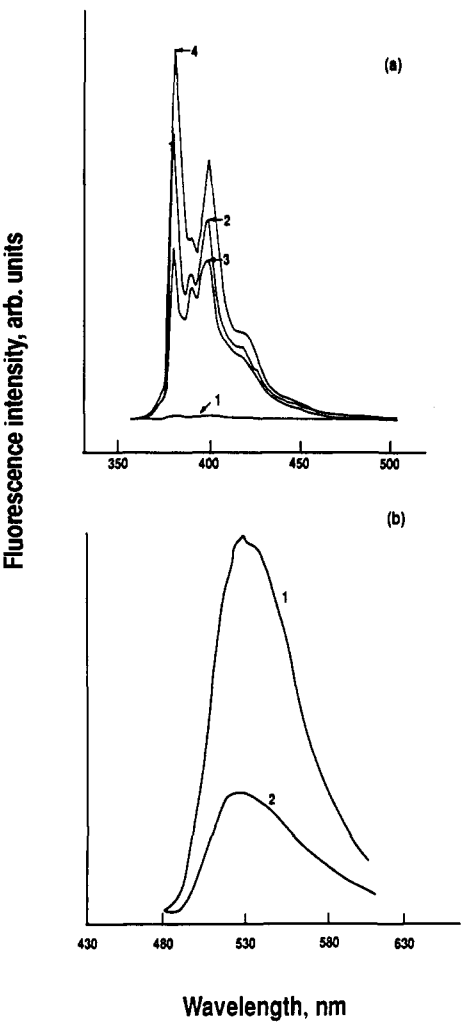

Figure 7. Upper: Modulation of the fluorescence intensity from a PS^- probe during redox switching of a PP/PS thin film (polymer thickness: ca. 0.3 μm). Spectrum 1 is for the polymer thin film at open-circuit; spectra 2–4 were obtained in sequence at potentials of −500, +500, and −900 mV, respectively. The excitation wavelength was 330 nm and the solution was 0.01 M TBAP in MeCN. Lower: Modulation of the fluorescence intensity from the acridine orange hydrochloride probe during redox switching of a PP/PSS thin film (polymer thickness: ca. 0.3 μm). Spectra 1 and 2 correspond to electrode potentials of +500 and −500 mV, respectively. The electrolyte in this case was 0.01 M NaPSS in H_2O, and the excitation wavelength was 480 nm. A dwell time of approximately 30 min was allowed at each potential prior to acquisition of the fluorescence data.

different potentials. These are steady-state experiments in that sufficient time (a few minutes) was allowed to elapse before initiating each wavelength scan at a given thin-film potential. Spectrum "1" is for the electrode at open-circuit. The absence of a noticeable solution signal is important and establishes that *spontaneous* ion exchange, i.e.

$$PP/PS + ClO_4^- \rightleftharpoons PP/ClO_4 + PS^- \quad (1)$$

is negligible on the time scale of these experiments. We had previously studied this process for the PP/OTs case;[42] it is typical of the spontaneous process to encompass a period of several hours. Electrochemical (potential) triggering of the redox electrochemistry initiates the ion fluxes at the PP/PS/electrolyte interphase (cf. spectra "2"–"4"). Thus, imposition of a potential of −500 mV reduces the poly(pyrrole) thin film. The PS^- species are consequently released and solution fluorescent activity ensues (spectrum "2"). On the other hand, reoxidation of the polymer (at a potential of +500 mV) results in the uptake of PS^- by the polymer and

(40) (a) Marque, P.; Roncali, J.; Garnier, F. *J. Electroanal. Chem.* **1987**, *218*, 107. (b) Roncali, J.; Garreau, R.; Yassar, A.; Marque, P.; Garnier, P.; Lemaire, M. *J. Phys. Chem.* **1987**, *91*, 6706. (c) Roncali, J.; Marque, P.; Garreau, R.; Garnier, F.; Lemaire, M. *Macromolecules* **1990**, *23*, 1347.

(41) Kalyanasundaram, K.; Thomas, J. K. *J. Am. Chem. Soc.* **1977**, *99*, 2039.

(42) Tsai, E. W.; Pajkossy, T. A.; Rajeshwar, K.; Reynolds, J. R. *J. Phys. Chem.* **1988**, *92*, 3560.

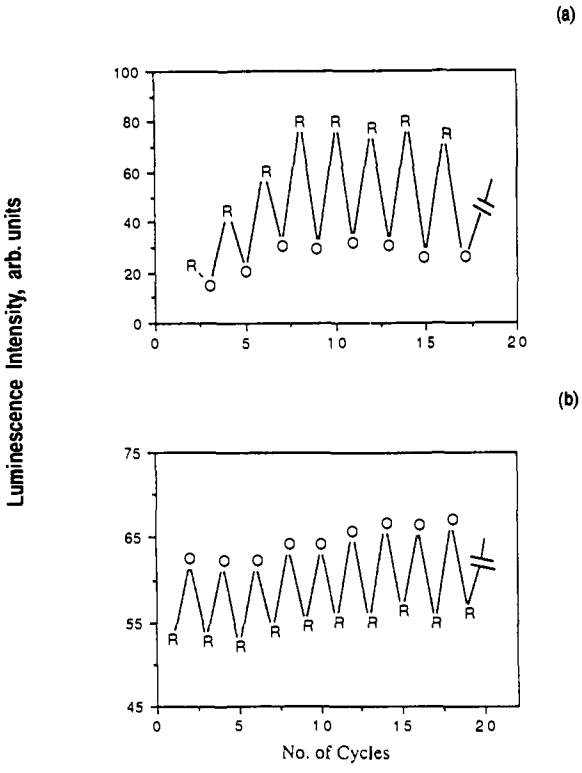

Figure 8. Upper: Modulation of the intensity of the 382-nm PS^- band of another PP/PS thin film (polymer thickness: ca. 0.3 μm) as the potential is repeatedly driven between the reduced state (R) at −900 mV and the oxidized state (O) at +500 mV. Lower: Similar experiment as in part a except that a PP/PSS film (polymer thickness: ca. 0.3 μm) was used in the pseudocathodic doping mode, and the 590-nm band of a $Ru(bpy)_3^{2+}$ probe was monitored with excitation at 440 nm. The electrolytes and other details are the same as in Figure 7.

consequent diminution of the fluorescent activity (spectrum "3"). The extent of release of the PS^- is proportional to the reduction potential as shown by spectrum "4" which was obtained at −900 mV. The influence of potential, however, is conveniently addressed in the scanning mode as detailed in a subsequent section.

The modulation of the fluorescent intensity is completely reversible after an initial "breakin" period as the data in Figure 8a demonstrate. The fluorescence emission intensities shown here were monitored at 382 nm for a +500 to −900 mV switching sequence for another PP/PS thin-film sample. Careful examination of the modulation data in Figures 7 and 8 allows the conclusion that the re-incorporation of the ejected PS^- back into the oxidized polymer phase is not complete, i.e., the emission intensity in the oxidation cycle does not return to zero. Obviously, this is a manifestation of the competitive uptake of both the PS^- and the (more abundant) ClO_4^- by the polymer on repeated cycles. In this regard, although the TBAP content of the solvent was reduced by one order of magnitude to ~0.01 M from the CV experiments, further lowering of solvent electrolyte content and inhibition of the ClO_4^- transport was precluded by the attendant iR drop problems.

Similar results as in Figures 7 and 8 were also obtained for the PP/NS thin films. For these samples, the fluorescence emission was scanned from 300 to 450 nm with excitation at 284 nm.

As mentioned in the Introduction, it is possible to "freeze" the anion motion via the use of an anionic polyelectrolyte such as PSS^-.[24] A PP/PSS thin-film sample thus synthesized was subsequently reduced at −900 mV in an aqueous solution containing ~0.1 M $Ru(bpy)_3Cl_2$. The reduced sample was thoroughly rinsed with water until the washings did not show the characteristic $Ru(bpy)_3^{2+*}$ emission.[43] The thin film was then reoxidized in

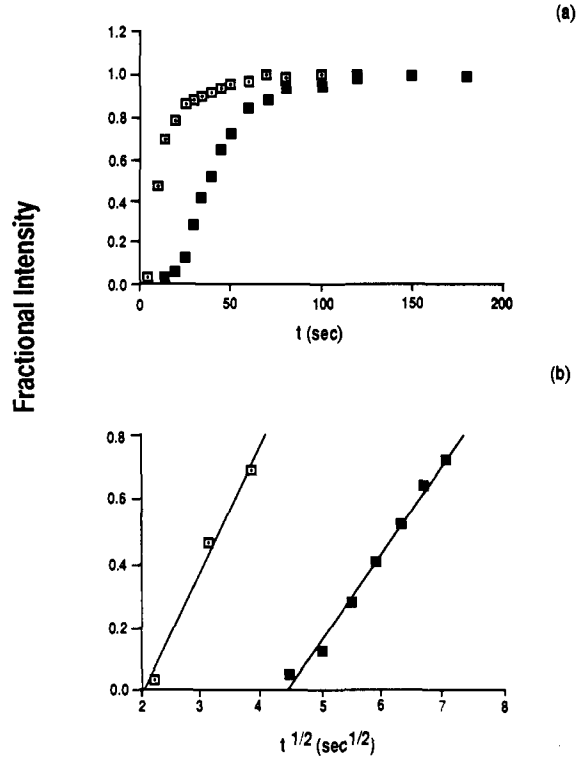

Figure 9. Upper: Growth of the intensity (expressed as a fraction, refer to text) of the 340-nm band of a NS^- probe from two different PP/NS samples of varying thickness [0.1 μm (□) and 0.6 μm (■) respectively]. The polymer potential was held at −850 mV in 0.01 M TBAP, MeCN. The excitation wavelength was 284 nm. Lower: Analyses of the data in part a in terms of fractional intensity vs $t^{1/2}$ plots. The symbols correspond in the two cases.

the spectroelectrochemical cell at 500 mV in a 0.01 M aqueous solution of NaPSS. Concomitantly, the emission monochromator was scanned from 550 to 675 nm with λ_{ex} set at 440 nm. The broad featureless $Ru(bpy)_3^{2+*}$ emission immediately appears signalling the expulsion of this specie from the oxidized polymer into the test solution (cf. Figure 1b). Again, the $Ru(bpy)_3^{2+}$ transport is reversible and stable as the modulation data in Figure 8b illustrate. These data pertain to the 600-nm-band intensity of the $Ru(bpy)_3^{2+}$ probe for a +500 to −700 mV switching sequence.

Acridine orange hydrochloride evinces similar pseudocathodic doping behavior. Figure 7b contains a sequence of fluorescence emission spectra for a PP/PSS sample which was prepared analogously to the $Ru(bpy)_3^{2+}$ case above. The λ_{em} was scanned between 490 and 625 nm with λ_{ex} set at 480 nm for this probe.[44]

Aside from ion transport studies, the fact that we are able to modulate the emission light intensity via control of an electrode potential (or equivalently, current) may itself have useful application possibilities. We had previously shown how electrochemical tuning of the luminescence quenching cross sections of a poly(pyrrole) thin-film surface leads to a light intensity modulation strategy.[23] The data in Figure 8 present a fundamentally different approach leading to analogous end results. It is also interesting to note that the polarities of the "ON-OFF" states for the two cases in Figure 8 are different, i.e. the fluorescence intensity is higher for a positive potential in Figure 8a whereas it is higher for a negative potential in Figure 8b. Such tuning of the modulation via changes in the chemical architecture of the PME is a novel aspect of these data.

The temporal aspects of the luminescence changes at the poly(pyrrole)/electrolyte interphase were probed in a preliminary fashion with use of PP/NS thin films of varying thickness. Figure 9a contains the data for two different film thicknesses. In these

(43) (a) Sutin, N.; Creutz, C. *Adv. Chem. Ser.* **1979**, *168*, 1. (b) Sutin, N. *J. Photochem.* **1979**, *10*, 19.

(44) Berlman, I. B. *Handbook of Fluorescence Spectra of Aromatic Molecules*, 2nd ed.; Academic Press: New York and London, 1971.

experiments, the potential was stepped from the first point to −850 mV while the emission intensity of the 340-nm band was monitored as a function of time. (The latter is expressed in terms of the fraction of the maximum emission intensity at "$t = \infty$" as is usual in kinetics representations.) The "S-shaped" nature of the plots in Figure 9a underlines the formal equivalence of the fluorescence monitoring to an electrochemical charge assay. This aspect will be further developed in the next section. For now, if we assume that membrane diffusion within the polymer phase is the predominant mode of mass transport (see below),[4] the data in Figure 9a may be analyzed via an approach described by previous authors.[16b] Thus, plots of the fractional intensity vs $t^{1/2}$ (analogous to a chronocoulometry or "Anson" plot, cf ref 45) are linear from the slopes of which the diffusion coefficient for ion transport, D_m, may be calculated. Such plots are shown in Figure 9b for the corresponding data in Figure 9a. A value for D_m of 10^{-10}–10^{-11} cm^2/s may be thus deduced. The variance between this value and those typical of mass transport in solution ($D = \sim 10^{-5}$ cm^2/s) assures that the rate control is exercised by transport through the polymer phase rather than through the bulk solution. Correspondingly, solution agitation had little influence on the temporal growth of the fluorescence signal.

Qualitatively, the trends in Figure 9 with the polymer film thickness are consistent with a membrane diffusion mechanism. Thus, thicker films have a higher degree of microporosity leading to consequently higher tortuosity in the pathways available to the egressing NS^- species from the polymer to the solution phase. The variation D_m with the polymer film thickness as observed in this study is also consistent with the trend observed by Penner et al.[29] While a simple diffusion model has been considered here, recent evidence suggests that intra-film diffusion processes in PME's [including poly(pyrrole)] may also involve migrational coupling complications as discussed by other authors.[3,46,47] In this regard, a systematic examination of variables that affect D_m such as the size of the potential step, solution composition, etc. has not yet been completed. However, another route to the examination of such effects is in situ luminescence monitoring of ion transport coupled with LSV; this is detailed next.

In Situ Luminescence Monitoring of Ion Transport Coupled with Linear Sweep Voltammetry of PP/NS Thin-Film Electrodes. A novel combination of LSV with luminescence measurements is described next, with the PP/NS system as a demonstration example. We will compare these results with those obtained via a UV–vis spectroelectrochemical method used previously by us for in situ monitoring of proton transport at poly(pyrrole) and RuO_x.[11,12] Figure 10 contains data from the potential-scanning technique. In experiments such as these, the PP/NS samples were removed from the polymerization medium at open circuit, thoroughly rinsed as before (cf. the CV section above), transferred to an appropriate medium (H_2O, 0.1 M $LiClO_4$ in this particular case), and scanned in the negative direction up to ~−700 mV. The positive-going cycle was not analyzed in these experiments because of the complications from the electrolyte species (see above).

The synchronization of the in situ fluorescence response and the cathodic current flow in Figure 10a is worthy of note. The differing curve shapes in the two cases are also entirely consistent with the cumulative nature of the former measurement and the rate information from the current response. Suitable calibration of the fluorescent response (see Experimental Section) coupled with use of the Faraday laws permits expression of this signal in terms of a corresponding charge equivalent. Differentiation of this then yields a current, i_{NS}, corresponding to the transport of

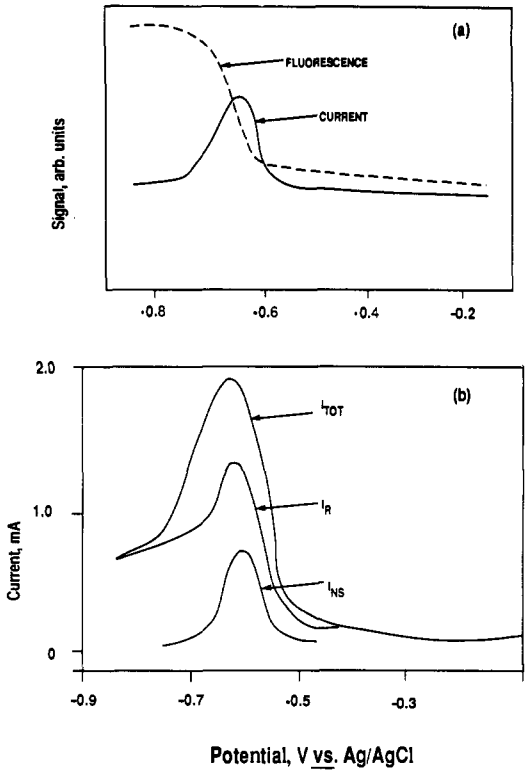

Figure 10. Upper: Combined in situ fluorescence–LSV experiment for a PP/NS thin film (polymer thickness: ca. 2 μm). The fluorescence emission was monitored at 340 nm (excitation: 284 nm) from the NS^- probe in 0.1 M $LiClO_4$ in H_2O. The potential san rate was 5 mV/s. Lower: Deconvolution of the total (measured) current, i_{TOT} (via procedures described in text), into the current due to the ejected NS^-, i_{NS}, and the residual component, i_R, for another PP/NS sample (polymer thickness: ca. 2.5 μm). The potential scan rate was 10 mV/s; other details are the same as in Figure 10a.

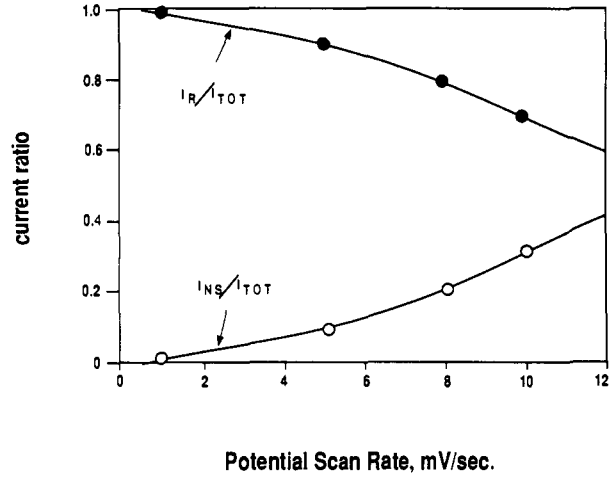

Figure 11. Variation of the contribution from i_{NS} and i_R to i_{TOT}, with the potential scan rate for 2 μm thick PP/NS thin-film electrodes. It must be noted that fresh samples were used to generate each data point in the figure. Other details are the same as in Figure 10.

NS^- species from the polymer phase to the solution where they are detected. Figure 10b shows the dependence of this parameter on the electrode potential. Also shown is the total (measured) current, i_{TOT} (as in Figure 10a), as well as a residual current, i_R, computed by using the additive nature of the two current components, i.e.

$$i_{TOT} = i_{NS} + i_R \quad (2)$$

The most surprising aspect of these data is that only a small fraction (a few percent, cf. Figure 11) of the injected cathodic current (or charge) results in the collection of NS^- in the solution

(45) Bard, A. J.; Faulkner, L. R. *Electrochemical Methods*; John Wiley: New York, 1980; Chapter 5, pp 199–206.
(46) (a) Yap, W. T.; Durst, R. A.; Blubaugh, E. A.; Blubaugh, D. D. *J. Electroanal. Chem.* **1983**, *144*, 69. (b) Elliott, C. M.; Redepenning, J. G. *Ibid.* **1984**, *181*, 137. (c) Doblhofer, K.; Braun, H.; Lange, R. *Ibid.* **1986**, *206*, 93. (d) Lange, R.; Doblhofer, K. *Ibid.* **1987**, *237*, 13. (e) Lange, R.; Doblhofer, K. *Ber. Bunsenges. Phys. Chem.* **1988**, *92*, 578. (f) Kaufman, J. H.; Mile, E. J.; Heeger, A. J.; Kaner, R.; MacDiarmid, A. G. *J. Electrochem. Soc.* **1983**, *130*, 571. (g) Paulse, C. D.; Pickup, P. G. *J. Phys. Chem.* **1988**, *92*, 7002.
(47) For example: *Faraday Disc. Chem. Soc.* **1989**, No. 88.

Table I. Parameters[a] for the Voltammetric Reduction of PP/NS Thin-Film Electrodes in 0.1 M $MClO_4$ (M = Li, K, Na, Cs)

cation	$-E_p$[b]	i_{TOT}[c]	i_{NS}[d]	i_{NS}/i_{TOT}[e]
Li	667 ± 21	0.51 ± 0.06	0.06 ± 0.03	0.12 ± 0.09
Na	627 ± 30	0.49 ± 0.05	0.08 ± 0.01	0.16 ± 0.03
K	685 ± 19	0.64 ± 0.09	0.14 ± 0.02	0.22 ± 0.04
Cs	732 ± 5	0.33 ± 0.09	0.02 ± 0.01	0.06 ± 0.03

[a] The mean and one standard deviation are reported from at least three replicate data sets in each case. [b] The peak potential in mV vs Ag/AgCl for the voltammetric reduction wave at 5 mV/s. [c] The peak voltammetric current for the reduction wave in mA. [d] The current due exclusively to NS^- transport (in mA) as determined from in situ fluorescence assay. [e] The uncertainty computed from the formula for error propagation in division.

phase. This fact may have serious implications in the practical use of electrodes such as PP/NS, e.g. in batteries.

Charge transfer kinetics limitations do not appear to be an underlying reason for this as the data in Figure 11 reveal (cf. also the CV data discussion). This figure shows the dependence of i_{NS}/i_{TOT} and i_R/i_{TOT} as a function of the potential scan rate (v) up to 0.010 V/s. (The use of higher scan rates was precluded by the constraints associated with the digitization of the fluorescent signal.) Interestingly enough i_{NS}/i_{TOT} *increases* with v (instead of showing the opposite trend expected for a charge transfer kinetics limited situation). The absence of a lag between the current response and the fluorescence signal (cf. Figure 10a) further argues against charge-transfer kinetics being an important factor. Rather, the trends in Figure 11 are better explained in terms of an electric-field enhancement of the diffusion of NS^- from the polymer to the solution phase (cf. ref 46f).

The fractional current efficiency for the transport of NS^- observed here is reminiscent of the situation with H^+ transport at poly(pyrrole) and RuO_x electrodes.[11,12] In these instances also, the charge corresponding to the protons "collected" via UV–vis spectroelectrochemical assays amounted to only a few percent of the total injected charge. Further, this fraction was dependent on variables such as the potential scan rate and the electrode morphology.

To further probe the origin of the discrepancy between i_{TOT} and i_{NS}, a series of experiments was conducted with PP/NS thin-film electrodes (synthesis charge: 49 mC) which were then voltammetrically scanned at 5 mV/s in the negative direction to ~−900 mV in 0.1 M perchlorate electrolytes containing Li^+, Cs^+, K^+, and Na^+, respectively. In each case, the fluorescence response also was simultaneously recorded as described above, and the data were processed as i_{NS}. Table I contains the results.

The ratio i_{NS}/i_{TOT} clearly is electrolyte cation dependent pointing toward the importance of parallel cation transport during the reduction of PP/NS thin films. Thus not only are the NS^- anions ejected from the polymer phase but the electrolyte cations are *simultaneously* injected from the electrolyte to maintain charge neutrality. The extent of these competing processes depends, aside from the nature of the electrolyte cation, on a variety of other factors including the potential scan rate (cf. Figure 11). It is also important to stress that these experiments address only the *first reduction cycle* for reasons alluded to above. Further, these data show how the "pure" anion and cation transport situations schematized in Figure 1 are obvious oversimplifications. The prevailing ion transport scenarios actually are more complicated as also discussed very recently by other authors for polybithiophene electrodes.[48]

Aside from our own previous work on poly(pyrrole), which was quoted above,[11] there is ample precedence for cation transport effects during redox cycling of conducting polymer electrodes. Thus, an earlier study employing the quartz-crystal microbalance revealed the uptake of Li^+ ions when poly(pyrrole) perchlorate thin films were reduced in tetrahydrofuran. Significant amounts of Cs^+ were also observed via XPS and atomic absorption spectroscopy when poly(pyrrole) thin-film electrodes were voltammetrically reduced in a variety of electrolyte/solvent combinations.[19] Our present data on PP/NS electrodes summarized in Table I show essentially similar trends. Correspondingly, XPS examination of voltammetrically reduced PP/NS in $CsClO_4$ and $NaClO_4$ showed noticeable growth of the 738- and 1071-eV Cs and Na signals relative to the parent (oxidized) state. Incidentally, we were unable to observe the Li 1s 55.5-eV signal in the reduced samples. We attribute this to the relative lack of XPS sensitivity to Li combined with the rather large hydration radius and the low ionic mobility of this cation (relative to Na^+, K^+, and Cs^+)[49] and the consequent propensity of proton transport when PP/NS is reduced in $LiClO_4$ (cf. ref 11).

Finally, we suppose that an oxidized poly(pyrrole) film releases the anions upon reduction via a moving boundary proceeding from the film surface inwards. Further anions are accelerated across the field generated within the insulating zone thus developed. A similar moving-boundary model has been developed and experimentally verified by Aoki et al.[30,50] for reduced poly(pyrrole). [The (conductive) zone movement proceeds outward in that case.] Vork et al.[33] have also considered very recently a model identical with ours in their discussion of anion effects on the properties of poly(pyrrole).

Concluding Remarks

The new in situ luminescence probe technique described herein has allowed us to address a number of issues related to mass transport during the redox electrochemistry of poly(pyrrole) thin-film electrodes. Within the overall context of ion transport at electrode/electrolyte interphases, a significant barrier to the development of new in situ probes is their ability to discriminate the ions undergoing egress/ingress from/into the electrode phase from the large quantities of (background) electrolyte species present. Further, the ion levels released from the polymer are rather small. This represents, in an analytical sense, an intrinsically unfavorable signal/noise situation. In this regard, luminescence techniques are very competitive relative to many other spectroscopic candidates in that they work best at trace levels of the analyte! Although the technique has been demonstrated here only for electronically conductive PME's such as poly(pyrrole), we anticipate logical extensions of this approach to encompass studies on other types of PME's, and indeed mass transport in any electrochemical situation in general. The key is the identification of an appropriate luminophoric probe for each particular scenario, and also preferably one which is electrochemically silent within the potential regime of interest.

The combined luminescence–LSV technique developed here is also novel and has not been used before in studies on PME's. Potential sweep techniques involving in situ monitoring of luminescence from electrode surfaces, however, have precedents in studies on electrode passivation phenomena.[51,52] In these studies, however, the light emission was from the (metallic) electrode surface itself, rather than localized in the solution as is the case in our technique. The term "cyclic fluorovoltammetry" has been suggested by previous authors[52] for the former approach.

Acknowledgment. This research was supported in part by the Defense Advanced Research Projects Agency (contract monitored by the Office of Naval Research). We thank John R. Reynolds for access to the thin-film profilometer, Kamal K. Mishra for assistance with the XPS measurements, and Peter Pickup for useful comments on an initial version of this manuscript. We also thank the two referees for prompting us to clarify our interpretation of the data in Figure 10.

(48) Hillman, A. R.; Swann, M. J.; Bruckenstein, S. *J. Electroanal. Chem.* **1990**, *291*, 147.

(49) Cotton, F. A.; Wilkinson, G. *Advanced Inorganic Chemistry*; John Wiley: New York, 1980; Chapter 7, p 255.

(50) (a) Aoki, K.; Tezuka, Y. *J. Electroanal. Chem.* **1989**, *267*, 55. (b) Tezuka, Y.; Aoki, K. *Ibid.* **1989**, *273*, 161.

(51) Perkins, R. S. *J. Electroanal. Chem.* **1979**, *101*, 47 and references therein.

(52) Rubin, J. C.; Gutz, I. G. R.; Sala, O. *J. Electroanal. Chem.* **1985**, *190*, 55.